Composite Mini-LED Backlight Packaging Structure with High Efficiency and Improved Uniformity

Po-Jui Chen[1], Chin-Chuan Wu[1], Chun-Ting Lin[4], Hung Tsou[4], Yi-Hsiang Huang[4], and Chung-Chih Wu[1,2,3]

[1]Graduate Institute of Electronics Engineering, National Taiwan University, Taipei, Taiwan

[2]Graduate Institute of Photonics and Optoelectronics, National Taiwan University, Taipei, Taiwan

[3]Depaertment of Electrical Engineering, National Taiwan University, Taipei, Taiwan

[4]Electronic and Optoelectronic System Research Laboratories, Industrial Technology Research Institute, Hsinchu, Taiwan

Abstract

This study explores diffraction and refraction composite structures in Mini-LED backlight modules, enhancing luminance uniformity and efficiency with a compact, micro-scale packaging design. Using a hybrid simulation of geometric and wave optics, the approach improves light distribution, optical performance, and carbon reduction, paving the way for broader Mini-LED adoption in various applications.

Author Keywords

Mini-LED backlight; Direct-lit; Packaging; High uniformity; High efficiency; Carbon reduction.

1. Objective and background

Mini-light-emitting diodes (mini-LEDs), with chip sizes ranging from 100 to 500 μm, have become popular as light sources for edge-lit and direct-lit LCD backlights. The compact dimension of mini-LED allows for local dimming, which provides precise control over brightness and high contrast ratio. This makes mini-LEDs ideal for achieving high dynamic range (HDR) and suitable for automotive and outdoor liquid crystal displays (LCDs). However, the point light nature of mini-LEDs leads to non-uniformity across the lighting area which significantly impacts the viewing quality of displays. Additional optical designs and components, such as diffusing films, brightness enhancement films (BEF), or other optical elements, are required to adjust the light distribution and to achieve higher uniformity.

Several design approaches can be employed to achieve high uniformity in mini-LED backlights. One method involves increasing the optical distance (OD) between the mini-LEDs and the optical films to extend the light mixing distance. Another method is to increase the number/density of mini-LEDs to reduce the spacing between chips. However, increasing the thickness and adding more LEDs conflict with the requirements for thin, lightweight, cost-efficient and energy-efficient advanced displays. Consequently, current solutions focus on incorporating secondary optical structures on the mini-LED to modify the light emission pattern.

Many studies have highlighted the importance of forming a "batwing" light distribution before light enters the diffusing film and BEF to improve uniformity [1]. For example, freeform lenses utilizing high-transmittance materials were placed on the mini-LED to alter the light emission pattern. Under conditions of 7.5 mm LED spacing and a 4 mm OD, efficiency greater than 90% and uniformity above 90% were achieved [2]. Other studies focus on reflective optical structures such as adding a semi-transmissive, semi-reflective diffuser layer above the mini-LED to reduce central intensity while enhancing wide-angle intensity [3]. The light field distribution can be further controlled by integrating reflective sidewalls between Mini-LEDs. [4].

The light field distribution can also be adjusted by reflective dot arrays of varying areas. The reflective dots near the center of the LEDs are larger, and gradually shrink as away from the center. This design allows more light to emit from regions farther away from the center [5]. Furthermore, optical films composed of high- and low-refractive index stacking layers, were introduced and directly coated onto the mini-LED surface. The transmission and reflection characteristics can be modified by adjusting the number of layers [6]. Such reflective thin film designs are typically thinner than transmissive optical structures but suffer from reduced efficiency due to material absorption.

There are also studies about minimizing transmissive optical structures to scales of hundreds or even tens of micrometers to reduce the device thickness. For instance, a phosphor quantum dot (QD) color conversion layer can be screen-printed to form microlens arrays, achieving 90% uniformity with a microlens thickness of only 24 μm [7]. Similarly, periodic microlens arrays with a 10 μm pitch and high transmittance have been shown to adjust the transmission and reflection distribution of light at the interface, achieving 85% uniformity with a structure height of 10 μm [8].

In this work, we proposed a composite, stepped-shape Mini-LED packaging structure that integrates freeform optical elements at both millimeter and 10-100 μm scales (i.e., lens and steps), enabling precise control of the emission profile while maintaining high efficiency. This composite packaging structure achieves higher uniformity at a 3 mm OD compared to a commercial automotive panel Mini-LED backlight having 7.5 mm mini-LED spacing. Based on the composite, stepped-shape architecture, two more optimized packaging structures are devised. By modifying specific elements to shapes better suited for directing light toward larger angle, the uniformity may be further improved, beneficial for reducing the number of Mini-LEDs required.

Finally, we investigate the impact of minimizing structures to the order of 10 μm. At these scales, diffraction effects emerge, causing deviations between geometric optics and wave optics simulation results. A hybrid simulation method was developed combining wave optics to model diffraction effects of the microstructure and geometric optics to simulate the overall packaging structure using bidirectional scattering distribution function (BSDF). By comparing results from geometric optics and the hybrid simulations, we found that diffraction effects can enhance backlight uniformity.

2. Results

Stepped-shape packaging structure optimization: The composite, step-shaped mini-LED packaging structure is shown in Figure 1. The stepped-shape design is constructed by placing right triangle elements (Figure 2(a), OS1) with a width of 0.1 mm along the x-direction on the truncated spherical surface with a radius of 2

ISSN 0097-996X/25/5601-0452-$1.00 © 2025

mm and a height of 1 mm. From the top view, the structure appears as a series of concentric circles. There is a total of 17 elements labeled by S1 to S17 from top to bottom. The configuration was adopted because their horizontal planes can redirect small-angle light to larger angles, while their vertical planes can redirect large-angle light to smaller angles. The combined effect suppresses the central intensity and enhances the intensity of light within the 20°–30° range. The overall width of the structure is about 3.4 mm, with a height of 1 mm, and the spacing between structures is 8.3 mm. The material of the structure is Silicone with a refractive index of 1.41, and the bottom is coated with 95% reflective Ag layer.

The packaging structure was simulated by geometric optics simulation (ray-tracing) software (LightTools). A 1 mm × 1 mm × 0.35 mm rectangle was used to represent a Mini-LED coated with a phosphor layer, with the Lambertian light source positioned at the top surface of the rectangle. The packaging structure was arranged in a 2×2 configuration. The far-field receiver was used to

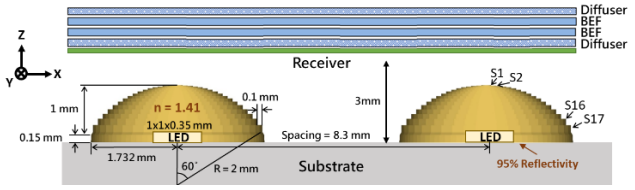

Figure 1. Schematic and parameters of the stepped-shape packaging structure.

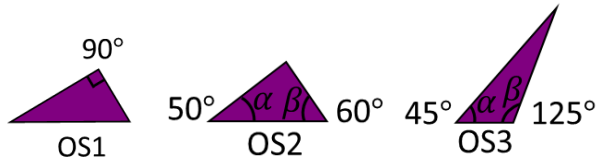

Figure 2. Schematic of component (a) OS1, (b) OS2, $\alpha = 50°, \beta = 60°$, (c) OS3, $\alpha = 45°, \beta = 125°$.

capture far-field intensity, and a planar receiver located 3 mm above the bottom of the structure was employed to record the illuminance entering the stacking of diffusing films and BEFs. The illuminance data were converted into uniformity using the following equations considering the logarithmic perception of brightness of the human eyes.

$$L_N(x,y) = Normalize\ L(x,y)\ to\ [0,256] \quad (1)$$

$$L_{log}(x,y) = \log(L_N(x,y)) \quad (2)$$

$$\begin{cases} L_{log}(x,y) = L_{log}(x,y),\ L_{log}(x,y) > 0 \\ L_{log}(x,y) = 0\ ,\ L_{log}(x,y) < 0 \end{cases} \quad (3)$$

$$Uniformity = \frac{L_{log,valley}}{L_{log,peak}} \quad (4)$$

$L(x,y)$ is the illuminance at position (x,y) of the receiver. $L_N(x,y)$ is the normalized $L(x,y)$. $L_{log}(x,y)$ is the logarithm of $L_N(x,y)$. $L_{log,peak}$ and $L_{log,valley}$ are the highest value on the receiver and the lowest value between two LEDs. First, the illuminance was normalized to $[0,256]$ then logarithmized. $L_{log}(x,y)$values below 0 were set to 0. Uniformity was calculated as the ratio of $L_{log,valley}$ divided by $L_{log,peak}$. Commonly, if the uniformity exceeds 75% before entering the diffusing film and the BEF, high luminance uniformity can be ensured after passing through these layers.

The simulated far-field and illuminance results of the stepped packaging structure are shown as the D1 configuration in Table 1. The far-field peak intensity occurs at 20°, with the central intensity suppressed, forming a valley. The ratio of the valley-to-peak intensity is 59.1%. The uniformity was calculated to be 75.5% under the LED spacing of 8.3 mm. Fewer LEDs are required compared to the commercial backlight design with a 7.5 mm LED spacing, beneficial for reducing manufacturing costs. Furthermore, since the structure is made of high-transmittance materials, the overall light-extraction efficiency reaches as high as 95%.

To further enhance uniformity, we analyze the far-field pattern of each element individually. Only the surface characteristics of one specific element were retained at a time and all other elements were set to absorb light. As shown in Figure 3, S1 to S6 fail to

Table 1. The schematic, far-field and 3 mm receiver Illuminance of D1, D2, D3 composite packaging structures (with 100 μm step period) and their cross-sections simulated by geometric optics simulation

Geometric Optics Simulation				
	D1	**D2**	**D3**	**Cross-section**
Schematic of S1-S6				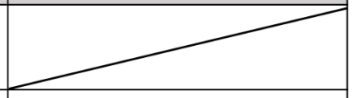
Far-field	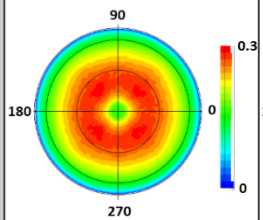	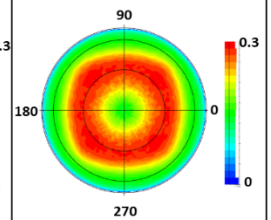	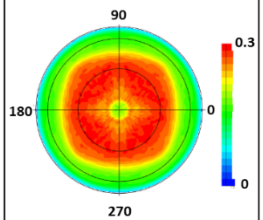	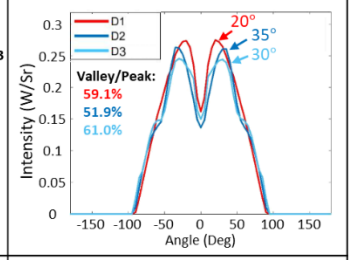
3 mm Receiver Illuminance (Log)	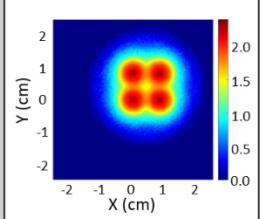	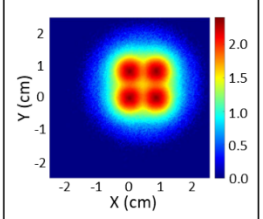	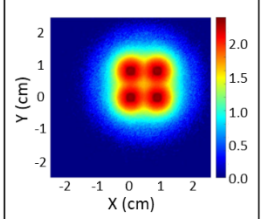	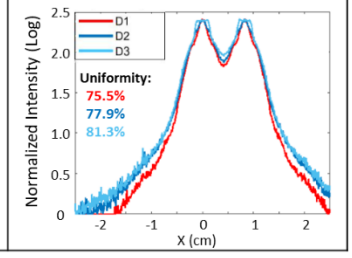

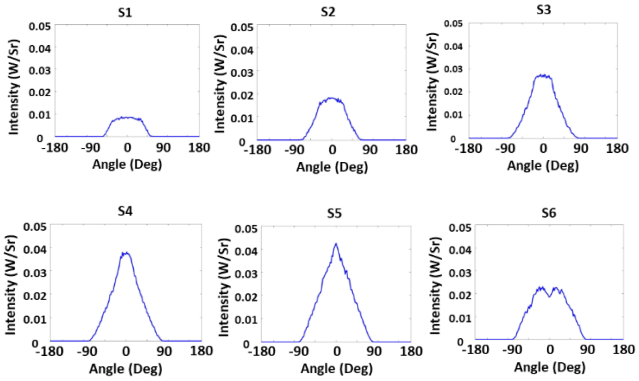

Figure 3. Far-field of S1-S6 using OS1.

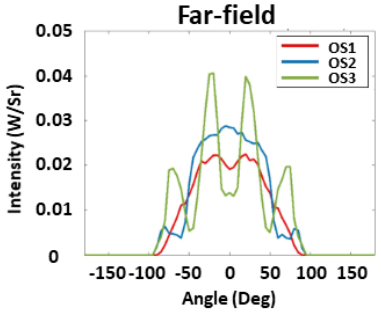

Figure 4. Far-field of S6 using OS1, OS2 and OS3.

direct light towards large angles. Therefore, the triangular elements of S1 to S6 were optimized by adjusting the angles α and β as shown in the Figure 2(b), 2(c). When α and β were set to 50° and 60° (OS2), as well as 45° and 125° (OS3), light could be directed towards larger angles. For instance, as shown in Figure 4, adopting the OS2 shape for S6 directs light towards angles greater than 50°, while adopting the OS3 shape for S6 directs light to 20°-30° and angles greater than 50°. Replacing S1-S5 with OS2 and OS3 yield similar effects. Consequently, improved D2 and D3 packaging designs were proposed. D2 uses OS2 for S1 to S6 and OS1 for S7 to S17, while D3 uses OS2 for S1 to S5, OS3 for S6, and OS1 for S7 to S17.

From the far-field and illuminance cross-section plots in Table 1, D2 directs the light to around ±30°, with the peak intensity at 35°. The ratio of the valley-to-peak intensity is 51.9%, and the uniformity is 77.9%. D3 also directs light to around ±30°, with the peak intensity at 30°. The ratio of the valley-to-peak intensity is 61.0%, and the uniformity is 81.3%. Both designs show an improvement in uniformity compared to D1, while also maintaining 95.7% and 95.8% light-extraction efficiency.

Hybrid simulation method for composite packaging structure with 10 µm periodic microstructure: We further studied smaller elements (steps) in the composite packaging structure and their impacts on light emission properties. When reducing the period of the structure in the x-direction from 100 µm to 10 µm, diffraction effects start to emerge, making pure geometric optics simulations insufficient to obtain realistic results. Therefore, wave optics simulation must be used. However, due to the large overall size of the packaging structure (3.4 mm x 1 mm), using wave optics alone is too time-consuming and memory-intensive.

Thus, a hybrid simulation combining wave optics and geometric optics was adopted. As shown in Figure 5(a), we employed the rigorous coupled-wave analysis method (RCWA, RSOFT DiffractMOD) to simulate the scattering characteristics of individual microstructures on the sphere at different incident angles to construct the BSDFs. The truncated sphere was then modeled in LightTools, divided into 17 layers in the z direction

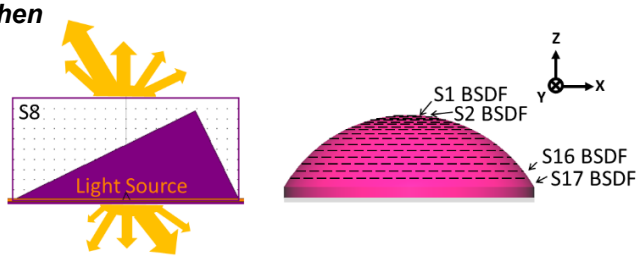

Figure 5. (a) RCWA modeling, (b) LightTools modeling of truncated sphere divided into 17 layers for BSDF.

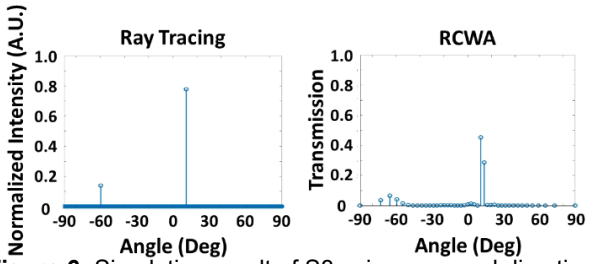

Figure 6. Simulation result of S8 using a normal direction light source by (a) ray-tracing, and (b) RCWA

based on the height of the 100 µm periodic elements. The BSDFs were assigned to each layer of the sphere (Figure 5(b)).

Two simplifications were made for the simulation. First, RCWA is designed for periodic structures. Although our microstructures are not entirely identical, the adjacent structures are highly similar. Additionally, at the size of 10 um, the interference between structures is not significant, and the diffraction mainly comes from the beam expansion effect caused by the size and shape of each microstructure. Thus, RCWA remains applicable and significantly reduces the simulation time compared to other wave optics simulations such as Finite-Difference Time-Domain method (FDTD).

Second, while a period of 10 um theoretically requires 170 layers, but as mentioned above, adjacent structures are nearly identical. Therefore, every 10 microstructures were represented by the central one (e.g., structure 1 to 10 are represented by the structure 5). Only 17 BSDFs were constructed to save simulation time.

The RCWA modeling is illustrated in Figure 5(a), focusing only on the microstructure above the sphere. The light source was positioned on the sphere's surface. The required resolution in the propagation direction, as well as the number of harmonics were tested. Higher resolution and more harmonics produce results closer to reality but at the cost of increased computation time and memory usage. Optimizing these parameters ensures simulation accuracy and efficiency. Figure 6 shows the results of S8 simulated by ray-tracing and RCWA respectively. Compared to ray-tracing, RCWA shows the clear beam expansion effect.

Next, D1, D2, and D3 packaging structures with step period of 10 um were simulated by the hybrid method. The simulation results are presented in Table 2. From the far-field plots, all three structures maintain the ability to direct light toward ±30°, with peak intensities at 25°, 30°, and 20°. The valley-to-peak ratios are 74.8%, 64.1%, and 76.3% respectively. In comparison with the ray-tracing results, due to diffraction, the emission pattern is broadened and more uniformly distributed within 10° and 40°angle range, reducing the valley-to-peak intensity difference and increasing the ratio. From the illuminance plots, the uniformity for D1, D2, and D3 are 74.4%, 79.0% and 81.8%, showing deviations of -1.1%, +1.1%, and +0.5% compared to the ray-tracing results. The uniformity difference might come from the trade off between the distribution broadening and valley-to-peak ratio increasing. The uniformity increases as more light be guided to larger angles by diffraction, and decreases as the valley-to-peak value becomes too high.

Table 2. The schematic, far-field and 3 mm receiver Illuminance of D1, D2, D3 composite packaging structures (with 10 μm step period) and their cross-sections simulated by geometric optics and wave optics hybrid simulation

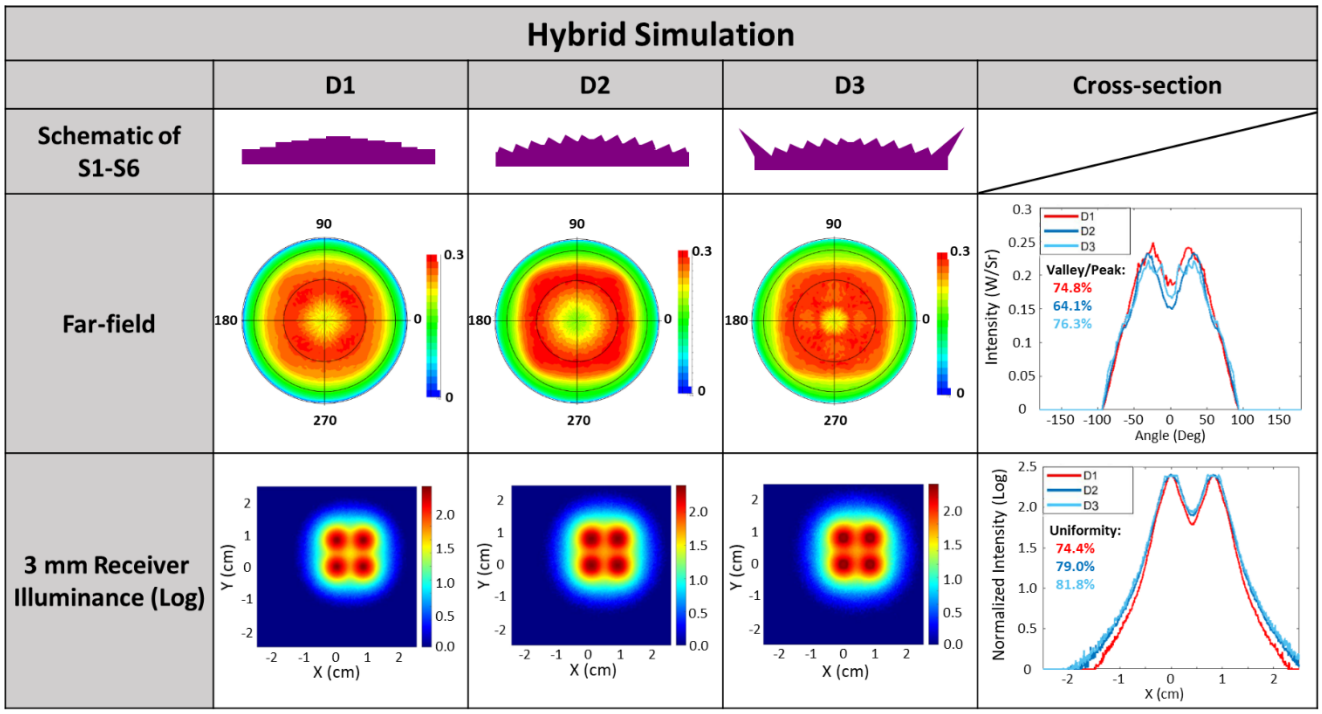

3. Impact

The uniformity of Mini-LED backlight determines the quality of the user's visual experience. Conventional methods to achieve high uniformity often rely on thick packaging structures or reflective materials with absorption, leading to bulky devices and increased power consumption. In this study, we present a novel composite, stepped-shape packaging structure and its variations, characterized by a compact form factor with a thickness of only 1 mm. These designs effectively guide light to larger angle forming a batwing far-field distribution. Compared to commercial Mini-LED backlight, the proposed approach enables wider LED spacing while maintaining a uniformity level exceeding 75% before entering the diffusing films and BEFs. In addition, taking advantage of the low refractive index and high transmittance properties of silicone, the packaging structure can achieve more than 95% light-extraction efficiency into the air.

To further understand the influence of shrinking structures on light distribution, a hybrid simulation combining geometric and wave optics was developed. This method uses BSDF to integrate the diffraction characteristics of microstructures into the geometric optics model, providing more realistic results for the complete packaging structure. We found that scaling down the structures can broaden the far-field distribution by diffraction, contributing to improved overall uniformity. This work for advanced Mini-LED backlight, optimistic to enhance optical performance and reduce carbon emission, paves the way for broader adoption of Mini-LED technology in consumer electronics, automotive displays, and other applications.

4. Reference

1. Zheng B, Deng Z, Zheng J, Wu L, Yang W, Lin Z, et al. An Advanced High-Dynamic-Range LCD for Smartphones. SID Symposium Digest of Technical 41-2. 2019.
2. Huang CH, Kang CY, Chang SH, Lin CH, Lin CY, Wu T, et al. Ultra-High Light Extraction Efficiency and Ultra-Thin Mini-LED Solution by Freeform Surface Chip Scale Package Array. Crystals. 2019 Apr 11;9(4):202.
3. Ye ZT, Hu CC, Zheng YJ. Wide heart-shaped mini-LEDs without a second lens as a large area, ultra-high luminance, and flat light source. Optics Express. 2024 Jan 24;32(4):5874–4.
4. Yamada M. Light - Emitting Device , Integrated Light - Emitting Device , and Light - Emitting Module. 2019.
5. Kikuchi S, Shibata Y, Takahiro Ishinabe, Hideo Fujikake. Thin mini-LED backlight using reflective mirror dots with high luminance uniformity for mobile LCDs. Optics Express. 2021 Jul 23;29(17):26724–4.
6. Xu L, Chuang Chia Ming, Li Y, Fan K, Zhang M, Sun H, et al. Uniform Illumination Realized by Large Viewing Angle of Gallium Nitride-Based Mini-LED Chip With Translucent Sublayer Pairs. IEEE access. 2021 Jan 1;9:74713–8.
7. Zhang W, Chen Y, Cai J, Deng L, Xu S, Ye Y, et al. Uniformity improvement of a mini-LED backlight by a quantum-dot color conversion film with nonuniform thickness. Optics Letters. 2023 Oct 6;48(21):5643–3.
8. Chen YL, Ye ZT, Lai W, Chiu CC, Lin KW, Han P. Application of Mini-LEDs with Microlens Arrays and Quantum Dot Film as Extra-Thin, Large-Area, and High-Luminance Backlight. Nanomaterials. 2022 Mar 21;12(6):1032–2.